V International Conference on Computational Methods in Marine Engineering
MARINE 2013
B. Brinkmann and P. Wriggers (Eds)

VIBRATION ANALYSIS OF PLATES WITH ARBITRARY STIFFENER ARRANGEMENTS USING A SEMI-ANALYTICAL APPROACH

LARS BRUBAK[*,a,b], JOSTEIN HELLESLAND[a] AND OLE J. HAREIDE[b]

[a]Mechanics Division, Department of Mathematics,
University of Oslo, 0316 Oslo, Norway

[b]Section for Ship Structures and Concepts, Technical Advisory
for Ship and Offshore Structures, Det Norske Veritas, 1322 Høvik, Norway

[*]e-mail: Lars.Brubak@dnv.com - Web pages: www.dnv.com and www.math.uio.no

Key words: Stiffened plates, Arbitrary stiffener orientations, Vibration analysis, Semi-analytical method, Rayleigh-Ritz method

Abstract. Vibration of plates with arbitrarily oriented stiffeners is studied. The plate may be subjected to in-plane loads and the plate boundaries may be simply supported or rotationally restained. The main objective is to present and validate an approximate, semi-analytical computational model for such plates subjected to in-plane loading. The formulations derived are implemented in a Fortran computer code, and numerical results are obtained for a variety of plate and stiffener geometries. The model may handle complex plate geometries, by using inclined stiffeners to enclose irregular plate shapes. The method allows for a very efficient analysis. Relatively high numerical accuracy is achieved with low computational efforts.

1 INTRODUCTION

Computationally efficient, semi-analytical methods are becoming more common as an alternative to finite element analyses (FEA) and explicit design formulas. The amount of published literature on semi-analytical methods for analysis of stiffened plates is growing. In a review paper by Liew, Xiang and Kitipornchai [1], most of the literature on vibration of stiffened plates till the year 1994 has been summarized. This literature study goes back to the well known study of vibration by Rayleigh [2] in 1877 and Ritz [3] in 1909. The latter approach is known as the Rayleigh-Ritz or Ritz method where a series of admissible trial functions are used. This approach is used in the present paper.

Semi-analytical methods such as the Rayleigh-Ritz approach and other mesh-less methods have been used to investigate many different aspect of vibration. For example, the

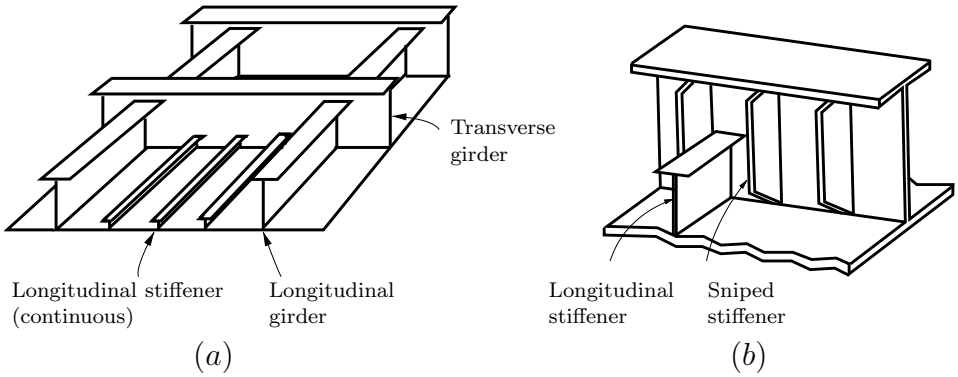

Figure 1: Examples of stiffened plates: (a) Stiffened plate enclosed by longitudinal and transverse girders, and (b) girder stiffened by sniped stiffeners.

Rayleigh-Ritz approach has been used to analyse free vibration of unstiffened plates with various boundary conditions [4, 5, 6], and vibration of plates subjected to in-plane loads [7, 8, 9]. Semi-analytical approaches have also been developed to investigate various aspects of vibration on stiffened plates [10, 11, 12, 13, 14]. In a research work by Xu, Du and Li [15], vibration of irregularly stiffened plates without in-plane loads is studied.

The semi-analytical methods mentioned above are restricted to irregularly stiffened plates without in-plane preloads, or to unstiffened or regularly stiffened plates. In the present work, the main objective has been to develop a computationally efficient semi-analytical model for eigenfrequency computations of stiffened plates subjected to in-plane prestress and with arbitrarily oriented stiffeners. Analyses by the present model can be performed for plates with simply supported, clamped of partially clamped boundary conditions, or combinations of these. The model may also handle interior supports, along lines with arbitrary orientations and lengths. By using inclined stiffeners or strong translational springs to enclose triangular, trapezoidal and other plate shapes, the present model may handle complex plate geometries.

2 PLATE DEFINITION AND BOUNDARY CONDITIONS

Typical engineering applications for stiffened plates are illustrated in Fig. 1(a) where a plate is enclosed by the strong longitudinal and transverse girders, and in Fig. 1(b) where the plate web is supported by a strong girder flange. Girder stiffeners may be be oriented horizontally or vertically. The stiffeners may be sniped at their ends (such as in Fig. 1(b)), and will then, unlike continuous stiffeners such as in Fig. 1(a), not be subjected to external axial loading (in the stiffener direction). Sniped stiffeners may also be used in conjunction with cases where a rather non-regular stiffener arrangement is required, such as for instance in the stern and in the bow of a ship hull.

In order to model such cases, the plate defined in Fig. 2 is considered. It may be subjected to in-plane shear stress and linear varying in-plane compression or tension stress. It may have none, one or more stiffeners, and the stiffener orientations may be

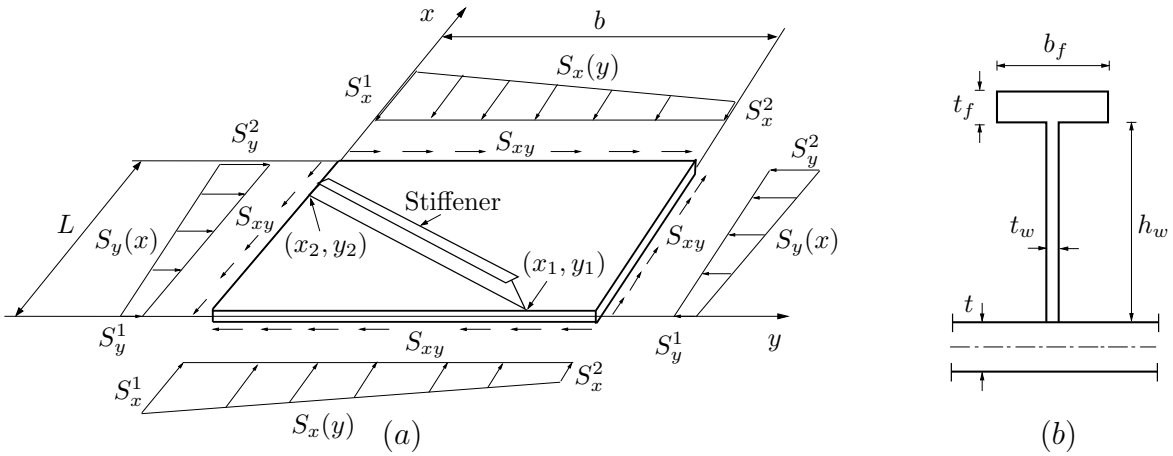

Figure 2: (a) Stiffened plate subjected to in-plane shear stress and in-plane, linear varying applied compression or tension stress, and (b) cross-section of an eccentric stiffener.

arbitrary. The stiffeners may have different cross-section profiles, and may be eccentric, as in Fig. 2(b), or symmetric about the middle plane of the plate. The stiffeners are modeled as simple beams. A boundary (plate edge) or a part of a boundary may be simply supported, clamped or something in between.

3 MATERIAL LAW AND KINEMATIC RELATIONSHIPS

The usual plane stress assumption for thin isotropic plates is adopted. The well known Hooke's law for this case is defined by

$$\sigma_x = \frac{E}{1-\nu^2}(\epsilon_x + \nu\epsilon_y) \tag{1}$$

$$\sigma_y = \frac{E}{1-\nu^2}(\epsilon_y + \nu\epsilon_x) \tag{2}$$

$$\tau_{xy} = \frac{E}{2(1+\nu)}\gamma_{xy} = G\gamma_{xy} \tag{3}$$

where σ_x, σ_y and τ_{xy} are the in-plane stresses, and ϵ_x, ϵ_y and γ_{xy} the in-plane strains, defined positive in tension, and the material coefficients E and ν are Young's modulus and Poisson's ratio, respectively. The total strain can be divided into a membrane strain (ϵ^m) and a bending strain (ϵ^b) and given by

$$\epsilon_x = \epsilon_x^m + \epsilon_x^b = \epsilon_x^m - zw_{,xx} \tag{4}$$

$$\epsilon_y = \epsilon_y^m + \epsilon_y^b = \epsilon_y^m - zw_{,yy} \tag{5}$$

$$\gamma_{xy} = \gamma_{xy}^m + \gamma_{xy}^b = \gamma_{xy}^m - 2zw_{,xy} \tag{6}$$

where w is the out-of-plane displacement in the z-direction (positive downwards in Fig. 2). The conventional notation $w_{,xy}$ for $\partial^2 w/\partial x\partial y$, etc., is adopted. The bending strain distribution complies with Kirchhoff's assumption [16].

4 VIBRATION ANALYSIS – EIGENVALUES

The eigenfrequencies of a perfect, stiffened plate are computed using the well known Rayleigh-Ritz method. The assumed displacement field, which satisfies the boundary conditions of a simply supported plate, is given by

$$w(x,y) = \sum_{i=1}^{M}\sum_{j=1}^{N} a_{ij}\sin(\frac{\pi i x}{L})\sin(\frac{\pi j y}{b}) \tag{7}$$

where a_{ij} are amplitudes, L the plate length and b the plate width.

By assuming harmonic vibrations, the usual eigenvalue problem [17] is

$$(K^M_{ijkl} + \Lambda^{pre} K^G_{ijkl} - \omega^2 M_{ijkl})a_{kl} = 0 \tag{8}$$

where

$$K^M_{ijkl} = \frac{\partial^2 U}{\partial a_{ij}\partial a_{kl}}\ ,\ \ \Lambda^{pre}K^G_{ijkl} = \frac{\partial^2 T}{\partial a_{ij}\partial a_{kl}}\ \text{ and }\ \omega^2 M_{ijkl} = \frac{\partial^2 H^{max}}{\partial a_{ij}\partial a_{kl}} \tag{9}$$

Here, ω denotes the natural circular eigenfrequencies and a_{kl} the corresponding eigenvectors. The desired prestress level is obtained by multiplying some initial (reference) applied in-plane stress by a load factor Λ^{pre}. In the eigenvalue problem, M is the mass matrix, K^M the material stiffness matrix and K^G is the geometrical stiffness matrix for the predefined in-plane stresses. These matrices are, as seen, expressed by U, T and H^{max}, which are the strain energy, potential energy due to external loads and the maximum kinetic energy, respectively. Each energy contribution is described in more detail below. In the common matrix notation, the eigenvalue problem above can be written

$$(\mathbf{K}^M + \Lambda^{pre}\mathbf{K}^G - \omega^2\mathbf{M})\mathbf{a} = \mathbf{0} \tag{10}$$

In an analysis of a clamped plate, it would be more appropriate to assume a displacement field defined with a series of cosine functions. However, although each component in a series of sine functions represents a simply supported condition, added together they are nearly able to describe a clamped, or partially restrained, condition at a negligible distance from the support. The sine curve assumption is therefore able to handle plates with various boundary conditions along the edges.

The elastic strain energy contribution from bending of the plate is given by

$$U^b_{\text{plate}} = \frac{D}{2}\int_0^b\int_0^L \Big((w_{,xx}+w_{,yy})^2 - 2(1-\nu)(w_{,xx}w_{,yy} - w^2_{,xy})\Big)\,dx\,dy \tag{11}$$

where $D = Et^3/12(1-\nu^2)$ is the plate bending stiffness and t is the plate thickness. By substituting the assumed displacement field, an analytical solution of this integral may be derived. More details can be found in Brubak [18] and Brubak, Hellesland and Steen [19]. The membrane strain energy of the plate and the stiffeners (below) is not included

as it does not affect computed eigenvalues, since small deflection theory is used. This will have some consequences that will be discussed in the results sections.

The curvature of the stiffeners is equal to the curvature in the plate along the stiffeners. Thus, the bending strain energy due to an arbitrarily oriented stiffener, with length L_s and cross-section area A_s, can be given by

$$U^b_{\text{stiff}}=\frac{EI_e}{2L_s^4}\int_{L_s}\left(L_x^2 w_{,xx}+2L_xL_y w_{,xy}+L_y^2 w_{,yy}\right)^2 dL_s \tag{12}$$

where (x_1, y_1) and (x_2, y_2) are the coordinates of the stiffener ends, $L_x = (x_2 - x_1)$, $L_y = (y_2 - y_1)$ and

$$I_e = \int_{A_s} (z - z_c)^2 \, dA_s + \, t \, b_e \, z_c^2 \tag{13}$$

is an effective moment of inertia about the axis of bending. Here, z_c is the distance from the middle plane of the plate to the centroidal axis (through the centre of area) of a cross-section consisting of the stiffener and an effective plate width b_e. The effective moment of inertia I_e reflects the fact that eccentric stiffeners tend to "lift" the axis of bending. For a symmetric stiffener, $z_c = 0$. This value also represents a reasonable simplification in many cases also for eccentric stiffeners. The strain energy integral in Eq. (12) may be solved analytically or by numerical integration. More details can be found in Brubak [18] and Brubak, Hellesland and Steen [19].

The potential energy of the external, in-plane prestress due to plate bending is given by

$$T = -\Lambda^{pre} \int_0^L \int_0^b \frac{t}{2}\left(S_{x0}(y)w_{,x}^2 + S_{y0}(x)w_{,y}^2 - 2S_{xy0}w_{,x}w_{,y}\right) dy \, dx \tag{14}$$

where $S_{x0}(y)$, $S_{y0}(x)$ and S_{xy0} are the initial (reference) stresses and Λ^{pre} the load factor for the prestress. More details can be found in Brubak [18] and Brubak, Hellesland and Steen [19].

The stiffeners in the example computations, presented below, are sniped. As a consequence, the in-plane stresses are applied at the midplane of the plate. Since the stiffeners will try to resist the corresponding strains, eccentricities (bending) will be introduced. However, such eccentricity effects are not accounted for in the model.

In line with the sniped stiffener assumption, Eq. (14) does not include any contribution from stiffeners. It would be reasonably straightforward to extend Eq. (14) to also include end loaded (continuous) stiffeners. However, in cases with local plate buckling, which are of most practical interest, the stiffeners will remain nearly straight and only contribute negligibly to T. Then it makes little difference whether the stiffeners are sniped or continuous. More details on how to include the energy contribution for end loaded stiffeners can be found in Brubak and Hellesland [20].

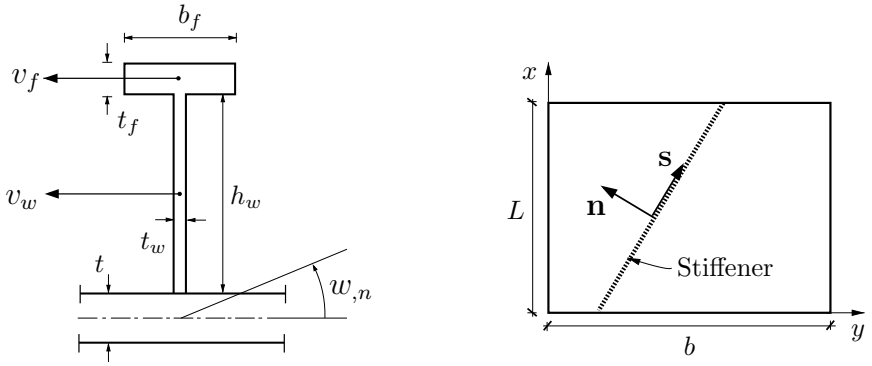

(a) (b)

Figure 3: (a) The velocity of the centroid of the web and flange due lateral displacement of the stiffener and (b) the stiffener orientation.

Both the displacements and the rotations along an arbitrary oriented line with length S may be restrained by applying translational and rotational springs, respectively. The strain energy due to these springs can be written

$$U_{\text{spring}} = \frac{1}{2}\int_S (k_r w_{,n}^2 + k_t w^2)\, dS \tag{15}$$

Here, $w_{,n}$ is the derivative of w normal to the line, and k_t and k_r are the stiffness of the translational springs and the rotational springs, respectively. More details can be found in Brubak [18] and Brubak, Hellesland and Steen [19]. Eq. 15 can also be applied for rotational springs at plate boundaries.

The maximum kinetic energy of the plate is given by

$$H_{\text{plate}}^{max} = \omega^2 \frac{\rho t}{2}\int_0^b \int_0^L w^2\, dx\, dy \tag{16}$$

where ρ is the density of the material, and the maximum kinetic energy of the vertical movement of the stiffener is given by

$$H_{\text{v,stiff}}^{max} = \omega^2 \frac{m_{st}}{2}\int_{L_s} w^2 dL_s \tag{17}$$

where $m_{st} = \rho(h_w t_w + b_f t_f)$ is the mass per unit length of the stiffener.

The kinetic energy of the rotational movement of the stiffener can be expressed by

$$H_{\text{r,stiff}} = \frac{1}{2}\int_{L_s} (m_w v_w^2 + m_f v_f^2) dL_s \tag{18}$$

where $m_w = \rho h_w t_w$ is the mass per unit length of the web and $m_f = \rho b_f t_f$ is the mass per unit length of the flange. As shown in Fig. 3(a), v_w and v_f is the lateral velocity of

the centroid of the web and the flange of the stiffener, respectively. By using geometrical considerations, these velocities can be written as

$$v_w = (0.5h_w + 0.5t)\frac{\partial w_{,n}}{\partial t} \quad \text{and} \quad v_f = (0.5t + h_w + 0.5t_f)\frac{\partial w_{,n}}{\partial t} \tag{19}$$

where $w_{,n}$ is the derivative of w normal to the stiffener orientation as illustrated in Fig. 3(b). By substituting Eq. (19) into Eq. (18), the expression for the maximum kinetic energy of the rotational movement of the stiffener can be written as

$$H_{\text{r,stiff}}^{max} = \omega^2 \frac{\bar{m}_{rot}}{2L_s^2} \int_{L_s} \left(L_y^2 w_{,x} + 2L_x L_y w_{,x} w_{,y} + L_x^2 w_{,y} \right) dL_s \tag{20}$$

where

$$\bar{m}_{rot} = m_w(0.5h_w + 0.5t) + m_f(0.5t + h_w + 0.5t_f) \tag{21}$$

The strain energy integral in Eq. (20) may be solved analytically or by numerical integration. The latter is used in the present work.

When all the expressions for the potential energy above are computed, the eigenvalue problem of Eq. (8) can be established and solved.

5 VALIDATION PREMISES

The present model was incorporated into a Fortran computer code and computed results have been compared with finite element analyses (FEA) using ABAQUS [21] for a variety of plate and stiffener dimensions, and in-plane prestress loads. Eigenfrequency results, presented as natural eigenfrequencies $f = \omega/2\pi$ [Hz], are verified by comparisons with FEA. Results, presented in subsequent sections, are limited to simply supported plates with sniped stiffeners.

The finite element model, based on shell elements (shell elements S4R both for plate and stiffeners), is supported in the out-of-plane direction along the edges of the plate, and the edges are forced to remain straight during deformation. The plate is also supported in the in-plane directions, just enough to prevent rigid body motions. Further, the ends of the stiffeners are completely free and not loaded (sniped).

The adopted elastic material properties in each computation are Young's modulus $E = 208000$ MPa and Poisson's ratio $\nu = 0.3$.

In the present model, 225 degrees of freedom (15x15) are used in all the cases. Comparable convergence studies carried out previously [19] have shown that this choice of degrees of freedom may overestimate the eigenfrequency predictions by, typically, about 1-2 %. In comparisons, the number of degrees of freedom used in the FEA analysis is typically about 20000, which is believed to be a sufficiently large number to ensure satisfactory results.

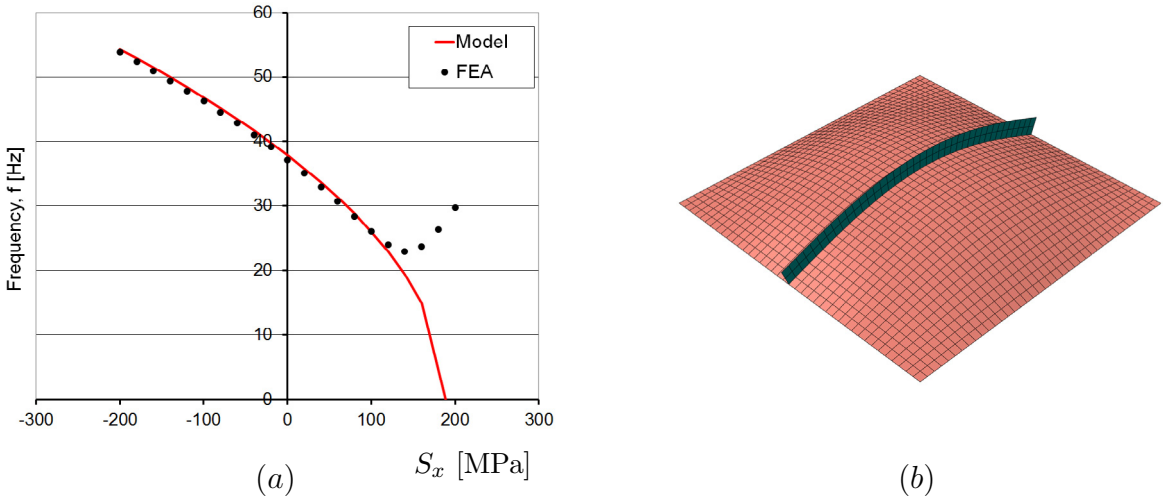

Figure 4: (a) Eigenfrequencies for a regularly stiffened plate subjected to uniaxial prestress S_x in the stiffener direction and (b) the eigenmode of the plate for free vibration.

6 REGULARLY STIFFENED PLATE WITH IN-PLANE PRESTRESS

Stiffened plates subjected to in-plane prestress have been analysed. A typical case is shown in Fig. 4(a), where the eigenfrequencies for a plate is computed for various magnitudes of prestress in the stiffener direction for both compression and tension. The plate ($L/b/t = 2000/2000/20mm$) is simply supported and is provided with one regular, sniped stiffener with a flatbar section ($h_w/t_w = 100/12mm$).

The agreement between the model and FE results is very good for external prestress smaller than about 120 MPa (Fig. 4(a)). This corresponds to about 63% of the elastic buckling stress, which has been found to be $S_{x,cr} = 189$ MPa in this case. Beyond this level, it can be seen that the model frequency results continues to decrease toward the elastic buckling stress (at the intersection with the S_x-axis) while the FEA results reaches a minimum value and then starts increasing for increasing prestress values. The reason for these differences is that the stiffness matrix in the FEA is computed using large deflection theory while the model is based on small deflection theory (in that the energy contribution from membrane strains does not affect the eigenvalues).

In large deflection theory, membrane stresses are redistributed from the interior of the plate fields to the stiffer parts, which are at the edges. This leads to a reduction in membrane compression stresses at the interior of the plate, which causes a larger eigenfrequency for the vibrations computed by FEA. It is worthwhile noting that this leads to solutions also for prestress values exceeding the classical elastic buckling stress. For plates without eccentricities (i.e., due to sniped stiffeners or imperfections), the membrane stress redistribution will start taking place at the classical buckling stress. With increasing eccentricities, the transition from the descending to the ascending portion of the frequency-prestress curve (FEA, Fig. 4(a)) becomes increasingly gradual. In the semi-analytical

	L	b	t	h_w	t_w
Plate 1	1200	2400	12	200	12
Plate 2	1600	2400	12	200	12

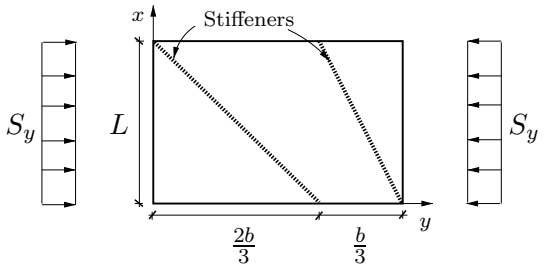

(a)

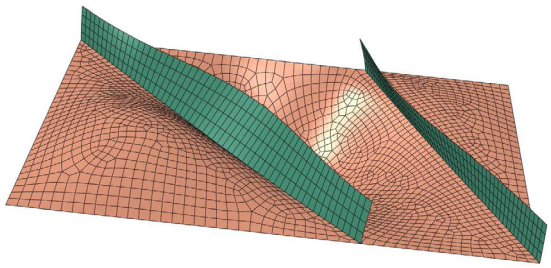

(b)

Figure 5: (a) Plate definitions and (b) eigenmode of Plate 1 subjected to prestress $S_y = 50$ MPa.

model, there is no redistribution of compression membrane stresses. Due to this, the frequency-prestress curve decreases continuously toward the elastic buckling stress. At and above this stress there is no solutions. In order to extend the model to include large deflection theory [22], it is expected that a similar formulation as in Brubak and Hellesland [23] for computing the post-buckling behaviour can be used.

The eigenmode for free vibration of the plate is shown in Fig. 4(b). This is a global mode where the stiffener deflection is one half wave. Similar modes with global deflections are also found when the plate is subjected to a prestress.

In its present form, application of the model should be limited to prestress values below about 60% of the classical elastic buckling stress for such cases, associated with global buckling modes and eccentric loads (sniped stiffeners). For local buckling modes such eccentricity effects are not that pronounced and the model will be able to handle prestress values closer to the elastic buckling stress (as shall be seen below).

7 IRREGULARLY STIFFENED PLATES

Typical results for two simply supported, irregularly stiffened plates defined in Fig. 5(a) are presented in Fig. 6 . The plates are provided with two inclined, eccentric stiffeners. The rather irregular stiffener locations are chosen such as to provide quite severe test cases for the present model. In this case, with a local eigenmode, the redistribution of compression stresses (discussed above) is less pronounced than above due to smaller eccentricity effects. This is reflected in the FEA results by a rather abrupt change in slope (sharp angle) for prestress values close to the elastic buckling stress. As already explained, the model does not reflect this phenomenon.

As seen (Fig. 6), the agreement between the model and the FE results is good for compression prestresses smaller than about 95% of the elastic buckling stress (as given by the intersection by the model results (full line) and the S_y-axis). For tensile prestress

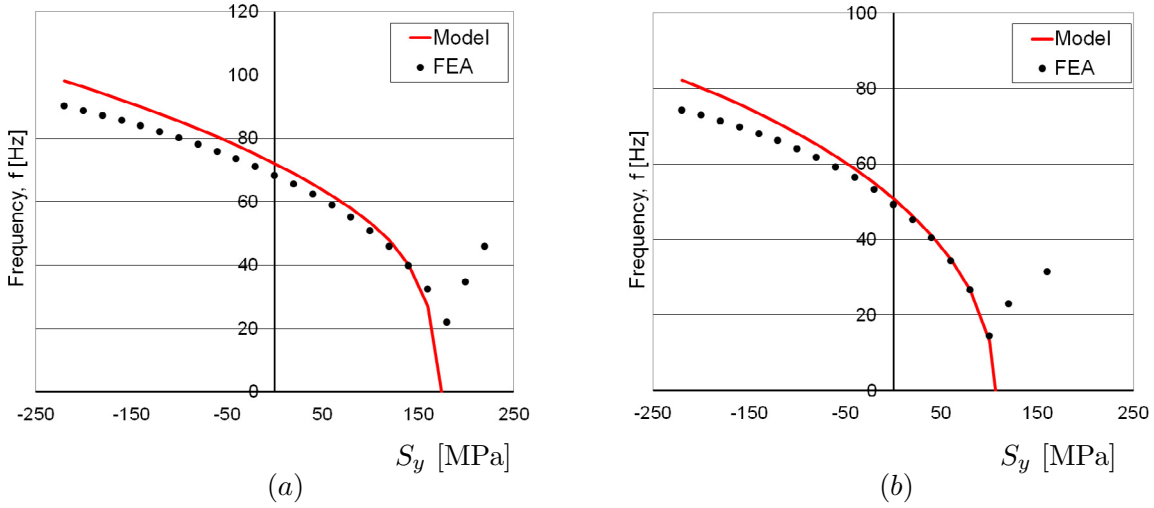

Figure 6: Eigenfrequency versus prestress S_y for (a) Plate 1 and (b) Plate 2.

values, the frequencies are somewhat overestimated, but still less than about 10% for prestress values as high as $S_y = -150$MPa. This is quite acceptable.

The shape of the first eigenmodes calculated by the present model and by FEA are quite similar in each case. Fig. 5(b) shows the first eigenmode of plate 2. This is a local mode with small out-of-plane deflections along the stiffeners.

8 CONCLUDING REMARKS

An efficient computational model for eigenfrequency computations of stiffened plates subjected to in-plane prestress with arbitrarily oriented stiffeners is presented, and results are obtained and compared with FEA results for cases with sniped stiffeners. The model is ideally suited in design optimisation studies and also in reliability studies that normally require a large number of case studies. A computer program based on this method is of a size that can easily be incorporated into a computerised design code. A minimal number of input parameters is required and the present model is therefore considerably more user friendly than commercial finite element programs, which requires experienced users to obtain reliable results.

Acknowledgments

The authors would like to thank dr. Eivind Steen at Det Norske Veritas (DNV), for his interest, suggestions and valuable discussions throughout the study.

REFERENCES

[1] K.M. Liew, Y. Xiang and S. Kitipornchai. Research on thick plate vibration: a literature survey, Journal of Sound and Vibration, 1995; 180(1): 163–176

[2] Lord Rayleigh. Theory of Sound. Volume 1, London: Macmillan; reprinted 1945 by Dover, New York, 1877

[3] W. Ritz. Über eine neue methode zur lösung gewisser variationsprobleme der mathematischen physik, Journal für Reine und Angewandte Mathematik, 1909; 135, 1–61

[4] J. Yuan and S.M. Dickinson. The flexural vibration of rectangular plate systems approached by using artificial springs in the Rayleigh-Ritz method, 1992, 159(1), 39–55

[5] R.B. Bhat. Natural frequencies of rectangular plates using characteristic orthogonal polynomials in Rayleigh-Ritz method, Journal of Sound and Vibration, 1985; 102(4), 493–499

[6] D.J. Dawe and O.L. Roufaeil. Rayleigh-Ritz vibration analysis of Mindlin plates, Journal of Sound and Vibration, 1980, 69(3): 345–359

[7] C.S. Kim, P.G. Young and S.M. Dickinson. On the flexural vibration of rectangular plates approached by using simple polynomials in the Rayleigh-Ritz method, Journal of Sound and Vibration, 1990; 143(3), 379–394

[8] O.L. Roufaeil and D.J. Dawe. Rayleigh-Ritz vibration analysis of rectangular Mindlin plates subjected to membrane stresses, Journal of Sound and Vibration, 1982; 85(2), 263–275

[9] M.M. Kaldas and S.M. Dickinson, Vibration and buckling calculations for rectangular plates subject to complicated in-plane stress distributions by using numerical integration in a Rayleigh-Ritz analysis, Journal of Sound and Vibration, 1981; 75(2), 151–162

[10] L.X. Peng, K.M. Liew, S. Kitipornchai. Buckling and free vibration analyses of stiffened plates using the FSDT mesh-free method, Journal of Sound and Vibration, 2006; 289(3), 421–449

[11] K.M. Liew, Y. Xiang, S. Kitipornchai, M.K. Lim Vibration of rectangular Mindlin plates with intermediate stiffeners Journal of Vibration and Acoustics, 1994; 116, 529–535

[12] R.B. Bhat. Vibrations of panels with non-uniformly spaced stiffeners, Journal of Sound and Vibration, 1982; 84(3), 449–452

[13] J.R. Wu and W.H. Liu. Vibration of rectangular plates with edge restraints and intermediate stiffeners Journal of Sound and Vibration, 1988; 123(1), 103–113

[14] M. Chiba and I. Yoshida. Free vibration of a rectangular platebeam coupled system, Journal of Sound and Vibration, 1996; 194(1), 49–65

[15] Hongan Xu, Jingtao Du and W.L. Li, Vibrations of rectangular plates reinforced by any number of beams of arbitrary lengths and placement angles, Journal of Sound and Vibration, 2010; 329(18), 3759–3779

[16] D.O. Brush and B.O. Almroth, Buckling of bars, plates and shells, McGraw-Hill Book Company, 1975

[17] A.K. Chopra, Dynamics of structures: theory and applications to earthquake engineering (third ed.), Prentice-Hall, 2007

[18] L. Brubak, Semi-analytical buckling strength analysis of plates with constant or varying thickness and arbitrarily oriented stiffeners. Research report in mechanics, No. 05-6, Norway: Mechanics Division. Dept. of Mathematics, University of Oslo; 2005. pp. 65

[19] L. Brubak, J. Hellesland and E. Steen. Semi-analytical buckling strength analysis of plates with arbitrary stiffener arrangements, Journal of Constructional Steel Research, 2007; 63 (4), 532–543

[20] Lars Brubak and Jostein Hellesland, Approximate buckling strength analysis of arbitrarily stiffened, stepped plates, Engineering Structures, 2007; 29(9), 2321–2333

[21] ABAQUS/Standard, User's Manual Version 6.7. volume Hibbitt, H. D. and Karlsson, B. I. and Sorensen, I. Hibbit, Karlsson and Sorenson Inc., Pawtucket; 2008.

[22] K. Marguerre, Zur theorie der gekrümmten platte grosser formänderung, Proceedings of The 5^{th} International Congress for Applied Mechanics, 1938; 93–101

[23] Lars Brubak, Jostein Hellesland. Semi-analytical postbuckling and strength analysis of arbitrarily stiffened plates in local and global bending, Thin-Walled Structures, 2007; 45(6), 620–633